Computing Redox Potentials in Solution: Density Functional Theory as A Tool for Rational Design of Redox Agents

Mu-Hyun Baik and Richard A. Friesner*

Department of Chemistry and Center for Biomolecular Simulation, Columbia University, New York, New York 10027

Received: March 28, 2002; In Final Form: May 29, 2002

High-level density functional theory in combination with a continuum solvation model was employed to compute standard redox potentials in solution phase for three different classes of electrochemically active molecules: small organic molecules, metallocenes, and $M(bpy)_3^x$ (M = Fe, Ru, Os; $x = +3, +2, +1, 0, -1$). Excellent agreement with experimentally determined redox potentials is found with an average deviation of approximately 150 mV when four different solvents commonly in use for electrochemical measurements were included. To obtain quantitative agreement between theory and experiment, the use of a large basis set is crucial especially when the redox couple includes anionic species. Whereas the addition of diffuse functions improved the results notably, vibrational zero-point-energy corrections and addition of entropy effects are less important. The computational protocol for computing redox potentials in solution, which has been benchmarked, is a powerful and novel tool that will allow a molecular-level understanding of the features dictating the properties of redox-active species.

I. Introduction

The standard redox potential, E^0, is a fundamental property of a molecule, one that is important in determining its chemical reactivity. Systematic measurements and extensive compilations of experimental data on electrochemically active species in condensed phase exist in the literature.[1−3] The knowledge of the characteristic potential of a redox pair at which electron transfer occurs can either be used as an analytical tool[4] or be exploited to promote often delicate chemical reactions in catalytic cycles.[5,6] The key to a number of important bioinorganic research directions, for example, elucidation of the catalytic cycle of metalloenzymes in their native environment and preparation of biomimetic constructs that are intended to reproduce enzymatic catalysis in an industrial setting,[8] lies in understanding and controlling the redox properties of the reactive species. Thus, the ability to accurately predict redox potentials for a given molecule in solution phase is highly desirable. Identifying key electronic features that dictate the redox potential on a molecular level is of substantial importance and might facilitate the derivation of rational strategies for tuning the redox properties of catalysts and provide a unique pathway to discovering novel redox-active systems with desired chemical behavior. Recently, a protocol similar to that discussed here was successfully utilized to scan hundreds of minimally functionalized pyrimidine bases searching for a system that would display an oxidation potential lower than that of guanine.[9] In that study, subsequent synthesis of the most promising candidate, 5-amino-cytosine, quantitatively confirmed the computational results for that species, thus confirming the validity of the approach.

In this paper, we examine the performance of state-of-the-art computational methods for predicting redox potentials in solution phase and give a systematic assessment of the required computational protocol for obtaining reliable results. Gas-phase ionization potentials of small molecules have often been used as standard benchmarks for quantum mechanical calculations,[10] and estimates for the typical errors for a given level of theory are established. For density functional theory (DFT)[11,12] at the B3LYP level,[13−17] the typical error has previously been determined to be in the range of 2 kcal mol^{-1}.[14] During the past decade, computationally efficient methods for self-consistently incorporating solvation effects have been introduced[18−20] that make use of a dielectric continuum to represent the bulk behavior of the solvent.[21−23] A convincing number of calculations on very different systems suggest that continuum solvation models give reasonable estimates for solvation energies with typical errors often ranging not more than a few kcal mol^{-1} (and often much less than this value if a serious parametrization effort is undertaken). Thus, the combination of DFT and the continuum solvation model is a promising platform for predicting redox potentials of molecules of substantial size in solution.

A few studies have appeared recently in the literature[24−29] that utilize similar approaches. The purpose of this account is to provide a benchmark and set the stage for studies currently underway in our laboratory targeting specific chemical questions that require the computation of redox potentials. Thus, one crucial requirement for the molecules considered in this study is that their redox potentials are known with a high degree of certainty. Many electrochemically active species undergo chemical side reactions on the same time scale as the electron-transfer process, introducing serious uncertainties regarding the accuracy of the measured potentials. We have thus selected three groups of molecules, shown in Scheme 1, for their well-known and reproducible redox behavior. In fact, many of the molecules that we study here are commonly employed as references to electrochemical experiments.[4]

The first series of molecules that we study (Scheme 1a) comprises simple organic molecules that span a remarkable potential range of approximately 3 V, reflecting the highly sensitive nature of the redox-active π-orbitals in these molecules toward functionalization. Similarly versatile is the electrochem-

10.1021/jp025853n CCC: $22.00
Published on Web 07/18/2002

SCHEME 1: Redox Active Systems Considered in This Study[a]

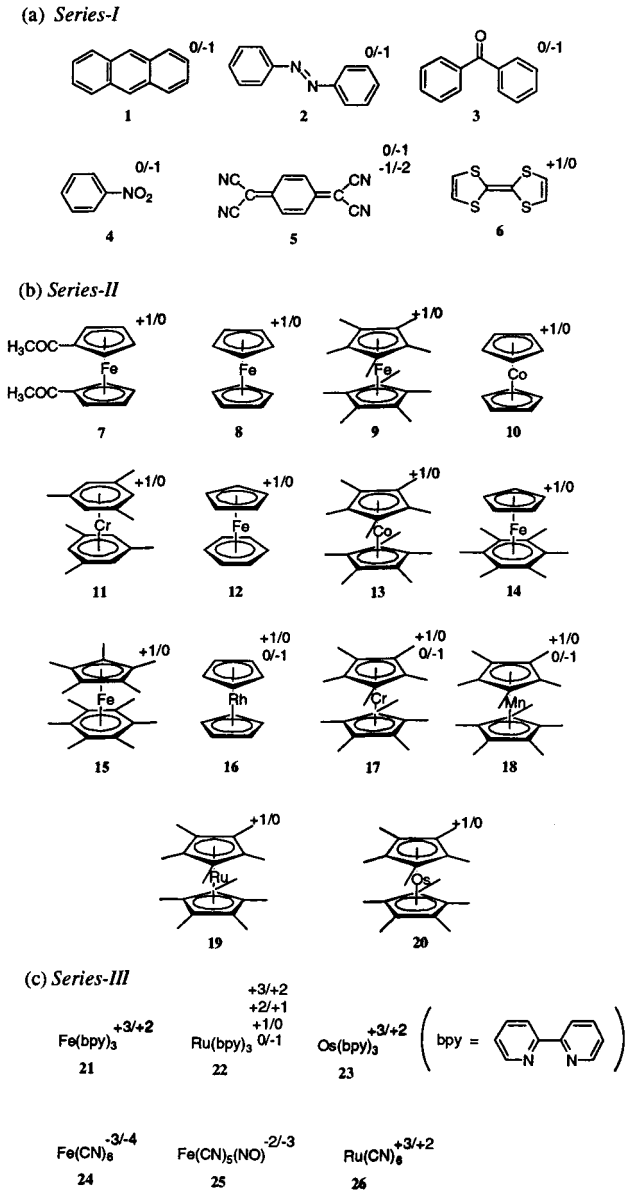

[a] Where more than two oxidation states are considered, the charges of all redox pairs are indicated.

istry of ferrocene and other metallocene complexes. The ability to reversibly and reproducibly undergo clean redox reactions[6] and the successful preparation of structurally well-defined polymeric structures to give interesting materials[30,31] have made metallocenes exciting candidates for serving as novel electron reservoirs. In addition, metallocenes are one of the most thoroughly studied class of molecules in modern electrochemistry.[6] Thus, we have included a series of metallocenes shown in Scheme 1b. The last series includes molecules of the type $[M(bpy)_3]^x$ (M = Fe, Ru, Os; $x = +3, +2, +1, 0, -1$; bpy = 2,2′-bipyridine) and three simpler mononuclear complexes, $Fe(CN)_6^{-3/-4}$, $Fe(CN)_5(NO)^{-2/-3}$, and $Ru(CN)_6^{-3/-4}$ (Scheme 1c). These classical inorganic complexes are of particular interest for a different project underway in our laboratory that aims at understanding the unique role of $M(bpy)_3$-type molecules in promoting water oxidation[32−34] and thus ultimately providing a starting point for devising a technical apparatus for artificial photosynthesis.[35]

Standard one-electron redox potentials, E^0, are related to the total electron attachment energy in solution, $\Delta G^{EA}(sol)$, by

$$\Delta G^{EA}(sol) = -FE^0 \quad (1)$$

where F is the Faraday constant. Computationally, $\Delta G^{EA}(sol)$ can be calculated routinely by computing the energy components.[36]

$$\Delta G^{EA}(sol) = \Delta G^{EA}(GP) + \Delta G^{solv} \quad (2)$$

$$\Delta G^{EA}(GP) = \Delta H^{EA}(GP) - T\Delta S(GP) \quad (3)$$

$$\Delta H^{EA}(GP) = \Delta H^{EA}(SCF) + \Delta ZPE + \Delta H^{T} \quad (4)$$

In our approach, the difference in free energy of solvation will be evaluated by numerically finding solutions to the Poisson−Boltzmann equations.[37] The remaining terms are readily obtained via gas-phase quantum chemical calculations, as is discussed below in more detail.

The paper is organized as follows. In section II, we describe the computational protocol for predicting the redox potentials, elucidating the various details of the methodology such as the basis sets employed at various stages, assessment of zero-point-energy effects, etc. Section III presents results for the three series discussed above, comparing computational and experimental results and discussing the implications of this comparison. Section IV, the conclusion, summarizes the results and considers future directions.

II. Computational Details

All calculations were carried out using DFT as implemented in the Jaguar 4.1 suite[38] of ab initio quantum chemistry programs. Geometry optimizations were performed with the B3LYP[13−17] functional and the 6-31G** basis set in which the transition metals are represented using the Los Alamos LACVP** basis[39−41] that includes relativistic effective core potentials. The energies of the optimized structures are reevaluated by additional single-point calculations on each optimized geometry using Dunning's correlation-consistent triple-ζ basis set[42] cc-pVTZ(-f) that includes a double set of polarization functions. For all transition metals, we used a modified version of LACVP**, designated as LACV3P**, in which the exponents were decontracted to match the effective core potential with the triple-ζ quality basis. Whereas the cationic and neutral species are likely sufficiently represented by these basis sets that include a double set of polarization functions, serious problems are expected for the anionic species. Thus, the single-point calculations were repeated with two sets of diffuse functions added, denoted as cc-pVTZ(-f)++ and LACV3P**++. Vibrational frequency calculation results based on analytical second derivatives at the B3LYP/6-31G**(LACVP**) level of theory were used to confirm proper convergence to local minima and to derive the zero-point-energy (ZPE) and entropy corrections at room temperature where unscaled frequencies were used. Note that by entropy here we refer specifically to the vibrational/rotational/translational entropy of the solute(s); the entropy of the solvent is implicitly included in the dielectric continuum model. The vibrational frequencies of all molecules in series I were computed. In series II, only the vibrational frequencies of ferrocene, **8**, and the ferrocenium ion, $\mathbf{8}^+$, were computed, and the ZPE/entropy corrections derived from these calculations were used for all other metallocenes. Similarly, the vibrational frequencies of all five ionic forms of $Ru(bpy)_3^x$ ($x = +3, +2, +1, 0, -1$) were computed[43] and also utilized for the iron and

osmium analogues. The ZPE/entropy corrections for each of the simpler systems, **24**−**26**, were computed. Although using the frequencies of a different molecule to estimate the ZPE/entropy correction is clearly unreliable even when the systems are closely related, the magnitude of the ZPE/entropy corrections suggests that this is only a minor effect (vide infra).

Solvation energies were evaluated by a self-consistent reaction field (SCRF)[18−20] approach based on accurate numerical solutions of the Poisson−Boltzmann equation.[37] In the results reported below, solvation calculations were carried out at the gas-phase geometry employing the dielectric constants[44] of $\epsilon = 80.37$ (water), 37.5 (acetonitrile), 36.7 (dimethylformamide), and 9.08 (dichloromethane). We considered recomputing the geometry with the SCRF potential applied self-consistently but decided after some experimentation to neglect structural relaxation due to the SCRF potential and use the solvation energy computed at the optimized gas-phase geometries. This approach provides a reasonable compromise between computational cost and model sophistication. As is the case for all continuum models, the solvation energies are subject to empirical parametrization of the atomic radii that are used to generate the solute surface. We employ the standard set[37] of optimized radii in Jaguar for H (1.150 Å), C (1.900 Å), N (1.600 Å), O (1.600 Å), and S (1.900 Å). For transition metals, we make use of the metallic van der Waals radii: Cr, 1.511 Å; Mn, 1.480 Å; Fe, 1.456 Å; Co, 1.436 Å; Ru, 1.481 Å; Rh, 1.464 Å; Os, 1.560 Å. In future work, we will investigate whether further optimization of these parameters would yield improved results; here, we simply report on the quality of the results obtained with no refitting to experimental data.

Experimental potentials are commonly reported as relative potentials referenced to a standard electrode with a specific potential. For the standard hydrogen electrode (SHE), the absolute potential has been determined experimentally to be 4.43 eV.[45] Instead of using the SHE, we chose to reference our computed potentials to the more commonly used standard calomel electrode (SCE). The standard potential of SCE is 0.2412 V more negative than that of SHE;[4] thus to compare the computed absolute potentials with the experimental potentials referenced to the SCE, 4.1888 V has to be subtracted.

III. Results and Discussion

It is convenient to define $\Delta H^{EA}(sol)$, which contains the electronic SCF energy difference of the redox pair in gas phase and the difference in free energy of solvation as computed in SCRF calculations.

$$\Delta H^{EA}(sol) = \Delta H^{EA}(GP) + \Delta G^{solv} \qquad (5)$$

This hybrid energy is rigorously not meaningful, because it contains the uncorrected enthalpic components of the solute only and the solvation free energy difference. The thermal corrections for the solute have to be added to give the true free energy difference, $\Delta G^{EA}(sol)$. However, $\Delta H^{EA}(sol)$ is the simplest approximation to the solution-phase electron attachment energy as available without any further calculations.[46] Figure 1 summarizes the B3LYP/6-31G** results of all three series of molecules both using the hybrid energy, $\Delta H^{EA}(sol)$, and using the ZPE/entropy-corrected free energy, $\Delta G^{EA}(sol)$, at room temperature where computed. The diagonal lines in Figure 1 correspond to perfect correlation. The values for the experimental and calculated redox potentials are collected in Table 1. It is noteworthy for future studies that the solvation energies are reasonably insensitive to basis-set size suggesting that

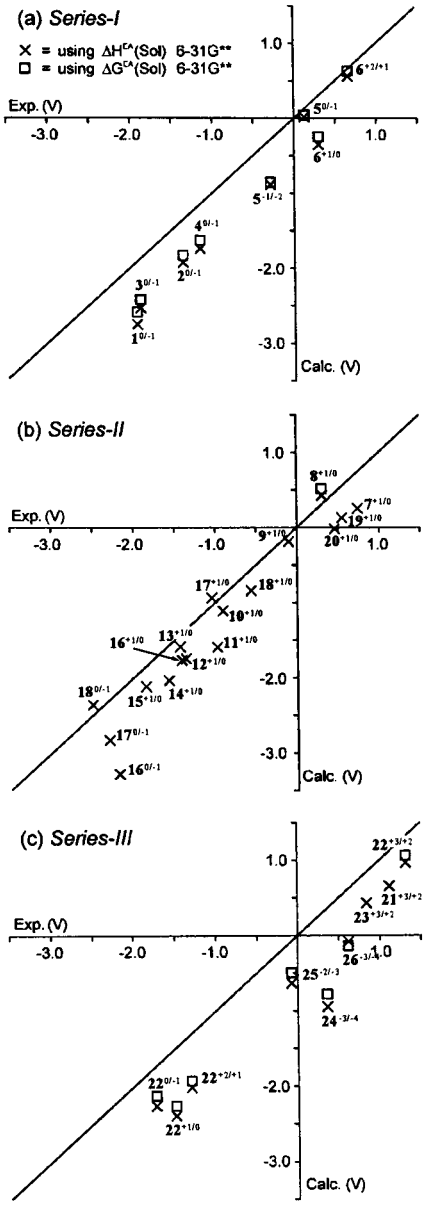

Figure 1. Correlation diagram of the experimental vs calculated redox potentials on the B3LYP/6-31G** level of theory with and without ZPE/entropy corrections.

recomputing them, as we have done here (see Supporting Information), when increasing the basis-set size is not necessary. The potentials derived using only $\Delta H^{EA}(sol)$ are of interest because the ZPE/entropy corrections require computationally very expensive vibrational frequency calculations that are out of reach for most of the interesting systems of realistic size. Thus, we wished to estimate the typical range of error that a complete neglect of these corrections would introduce.

The computed absolute potentials based on $\Delta H^{EA}(sol)$ shown in Figure 1 give the correct overall trend, but the agreement with experiment is not satisfactory. The addition of the ZPE/entropy corrections (corrected potentials are plotted as squares in Figure 1) does not improve the results significantly, although the corrections have the correct sign in all cases where notable contributions are determined. The average of the correction is +0.09 V with the maximum seen for the redox pairs $\mathbf{1}^{0/-1}$ (anthracene) and $\mathbf{24}^{-3/-4}$ ($Fe(CN)_6$), for which the differential ZPE/entropy energy amounts to +0.166 V. Given the diversity in structure and charge of the redox pairs examined, these results suggest that the ZPE/entropy corrections can be considered

TABLE 1: Calculated Redox Potentials Based on ΔG^{EA}(sol)

	solvent[a]	charge	E^0 (exptl)	E^0 (calcd) 6-31G**	E^0 (calcd) cc-pVTZ(-f)	E^0 (calcd) cc-pVTZ(-f)++
1	DMF	0/−1	−1.92[4]	−2.591	−2.173	−2.138
2	DMF	0/−1	−1.36[4]	−1.833	−1.437	−1.335
3	AN	0/−1	−1.88[4]	−2.426	−1.985	−1.822
4	AN	0/−1	−1.15[4]	−1.633	−1.228	−0.983
5	AN	0/−1	+0.13[4]	0.041	0.240	0.333
5	AN	−1/−2	−0.29[4]	−0.855	−0.524	−0.377
6	AN	+2/+1	+0.66[4]	0.628	0.594	0.623
6	AN	+1/0	+0.30[4]	-0.246	-0.143	0.465
7	DMF	+1/0	+0.74[6]	0.340	0.364	0.355
8	AN	+1/0	+0.31[6]	0.517	0.573	0.425
9	DMF	+1/0	−0.10[6]	−0.098	−0.089	−0.053
10	DMF	+1/0	−0.91[6]	−1.019	−1.060	−1.002
11	DMF	+1/0	−0.98[6]	−1.500	−1.357	−1.351
12	DMF	+1/0	−1.36[6]	−1.658	−1.651	−1.608
13	DMF	+1/0	−1.43[6]	−1.497	−1.606	−1.581
14	DMF	+1/0	−1.57[6]	−1.945	−1.955	−1.824
15	DMF	+1/0	−1.85[6]	−2.027	−1.963	−1.911
16	AN	+1/0	−1.41[6]	−1.677	−1.348	−1.259
16	AN	0/−1	−2.18[6]	−3.192	−2.649	−2.455
17	AN	+1/0	−1.04[6]	−0.845	−0.886	−0.910
17	AN	0/−1	−2.30[6]	−2.739	−2.561	−2.463
18	AN	+1/0	−0.56[6]	−0.749	−0.451	−0.509
18	AN	0/−1	−2.50[6]	−2.272	−2.386	−2.252
19	CH_2Cl_2	+1/0	0.55[6]	0.217	0.562	0.594
20	CH_2Cl_2	+1/0	0.46[6]	0.072	0.483	0.443
21	H_2O	+3/+2	+1.12[1]	0.744	0.664	0.638
22	AN	+3/+2	+1.32[4]	1.057	1.101	1.084
22	AN	+2/+1	−1.30[4]	−1.923	−1.733	−1.715
22	AN	+1/0	−1.49[4]	−2.257	−2.110	−2.046
22	AN	0/−1	−1.73[4]	−2.125	−1.848	−2.337
23	H_2O	+3/+2	+0.84[1]	0.518	0.640	0.636
24	H_2O	−3/−4	+0.36[1]	−0.778	−0.427	−0.199
25	H_2O	−2/−3	−0.07[1]	−0.499	−0.337	−0.172
26	H_2O	+3/+2	−0.03[1]	−0.141	0.085	0.422

[a] DMF = dimethylformamide; AN = acetonitrile.

second-order effects. Complete neglect of these terms would not have afforded a qualitatively different result in the examples chosen here.

In the case of the organic molecules in series I, a systematic error is observed that gives rise to an almost consistent shift of all potentials by roughly −0.5 V, except for the redox pairs $\mathbf{5}^{0/-1}$ and $\mathbf{6}^{+2/+1}$, for which errors of −0.09 and −0.03 V are observed, respectively. The most serious errors are associated with potentials that involve anionic species with a maximum error as large as −1.14 V for the anionic couples $\mathbf{24}^{-3/-4}$. Similarly severe problems are encountered for the sandwich complex couple $\mathbf{16}^{0/-1}$, which involves a neutral and a monoanionic species. Disagreement between theory and experiment of such magnitude poses some serious concern about the usability of the protocol in a realistic setting. However, the next set of calculations on the B3LYP/cc-pVTZ(-f) level of theory gives dramatic improvements. The average absolute deviation of the redox potentials for the molecules of series I decreases upon use of the cc-pVTZ(-f) basis set from 0.425 to 0.171 V and decreases further to 0.120 V when diffuse functions are added. The latter translates to an error of 2.8 kcal mol^{-1}, which approaches the accuracy limit established for DFT. Similar improvements are observed for the metallocene complexes of series II. The average deviation decreases from 0.307 V at the 6-31G** level to 0.196 and 0.165 V at the cc-pVTZ(-f) and cc-pVTZ(-f)++ levels of theory, respectively.

On a first glance, the improvements seen for the third series is less satisfactory. The average absolute deviation is 0.563 V at the 6-31G** level and remains quite large at 0.420 and 0.372 V on the higher levels, respectively. However, as Figure 2c demonstrates clearly, all potentials of the molecules in series III are systematically shifted. The rms value for the linear extrapolation is 0.9844 at the cc-pVTZ(-f)++ level, and Figure 2c demonstrates that the theory−experiment correlation is in the same order of magnitude as that seen for the first two series if the baseline shift is taken into account. Most importantly, the computed potentials of $Ru(bpy)_3^x$ become consistent to each other at the cc-pVTZ(-f)++ level. To be useful in practice, it is crucial that the computational method reproduces the relative ordering of redox potentials. In the $Ru(bpy)_3^x$ series, the potentials become successively more negative with decreasing formal oxidation state of Ru. Both at the 6-31G** and at the cc-pVTZ(-f) level, the computed potential for the neutral and the anionic couple $\mathbf{22}^{0/-1}$ is too positive compared to those of the three other possible redox pairs of **22**. Thus, a wrong ordering of the potentials is predicted, which has dramatic implications for the redox reaction studied. In fact, such a situation in which the reduction potential of the 0/−1 pair is more positive than that of the +1/0 couple is known as

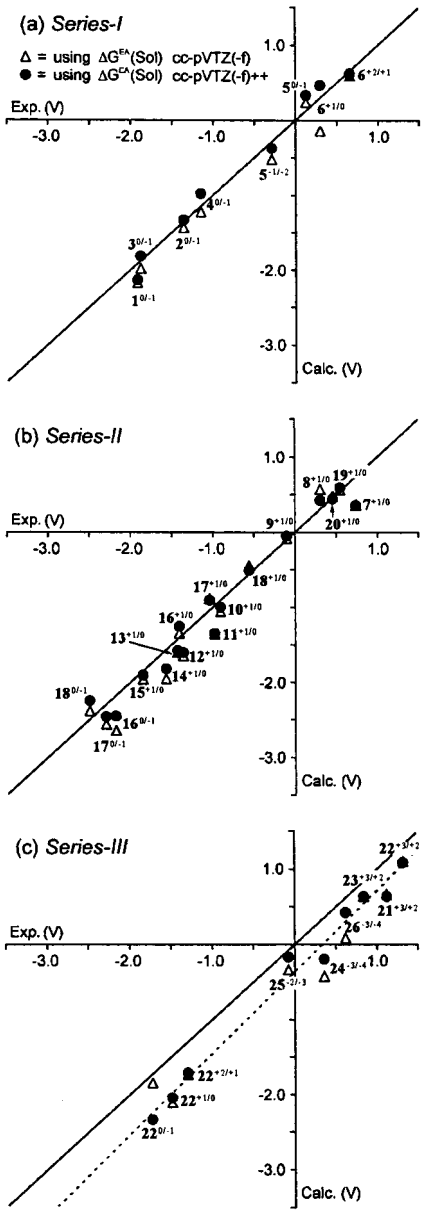

Figure 2. Correlation diagram of the experimental vs calculated redox potentials on the B3LYP/cc-pVTZ(-f) and B3LYP/cc-pVTZ(-f)++ levels of theory (ZPE/entropy-corrected).

"inverted-potentials" and implicates the intrinsic instability of the neutral species with respect to disproportionation[29] leading to a very misleading and different interpretation of the redox behavior. The use of cc-pVTZ(-f)++ recovers the correct ordering and gives an excellently correlated relative ordering. Note, that the correlation of the four computed potentials of the $Ru(bpy)_3^x$ with experiment forms a perfect line. This observation confirms the widely recognized importance of using diffuse functions when anions are involved. $Ru(bpy)_3^{-1}$ is clearly an extreme case, however, because it is formally a 21-electron complex enforcing a highly frustrated electronic structure that requires a large basis set for an accurate representation. The systematic shift of the potentials computed for the molecules of the series III is likely due to a systematic overestimation of the solvation energy with increasing positive charge, as the slope of the linear correlation line indicates. Such a systematic baseline shift is an expected result and reflects the mismatch of the solvation model parameters with the systems studied. Thus, it is not surprising that the best predictions are obtained for the series of organic molecules more related to the training set[20] that had been used to derive the solvation parameters.

Reliable experimental solvation energies for transition metal complexes are rare and thus there are currently no solvation models available that are systematically optimized for transition-metal-containing systems. The flexibility in oxidation states, charges, and ligand coordination geometry commonly encountered at transition metal centers reflecting a wide range of possible electronic structures poses a serious challenge to empirical methods that rely on the similarity of the atoms in different molecular structures. In addition to likely diverse charge distribution patterns at the metal center depending on the ligand environment, the metal−ligand interaction itself can also be dramatically different giving rise to a very untypical electron distribution on the ligand when compared to the free ligand molecule. Because in many cases the metal centers are buried inside the solute cavity, which is primarily defined by the ligand moieties, the use of unoptimized transition metal radii is not expected to be a major source of error. However, it is intuitively clear that, for example, the use of radii for hydrogen, carbon, and oxygen that are fit to reproduce the free energy of solvation of relatively simple organic species is a priori inappropriate for ligands that interact strongly with the transition metal. Thus, fitting the solvent−solute interaction behavior of the metal-containing systems of series II and series III with a single set of dielectric radii is likely to introduce systematic errors. A possible method to deal with this intrinsic problem of the parametrized solvation model is to introduce a scaling factor for the solute atomic radii as a function of the atomic charge determined in gas-phase calculations. Further examination of this and other possible technical improvements to obtaining solvation energies that are in better agreement with experimental redox potentials is currently in progress in our laboratory.

Optimizing continuum solvation energy calculations of organometallic complexes indirectly by making use of the redox potential calculation protocol discussed in this paper is a promising alternative to usual small-molecule fitting procedures and gives access to an extensive database of well-established experimental data. Given the fundamental difficulties mentioned above and the fact that our study included four different solvents, the agreement between theory and experiment is highly satisfactory. Clearly, error cancellation of the absolute solvation energies to yield an acceptable differential solvation energy that enters the redox potential calculation must be operative.

IV. Conclusions and Outlook

We have examined the performance of a straightforward and intuitive theoretical protocol to compute redox potentials in solution phase, which is adding the differential solvation energy of the redox couple calculated using a continuum solvation model to the gas-phase electron attachment energy of a DFT calculation, on three different series of molecules that have practical relevance to electrochemical research. Our results suggest that only moderate agreement between experiment and theory is achieved when the standard basis set 6-31G** is used in combination with the popular B3LYP functional. However, if the more sophisticated cc-pVTZ(-f)++ basis set is used, the agreement between computed and experimentally determined redox potentials is excellent. The addition of ZPE and entropy corrections give, in principle, an improvement of the results, but the effects are only minor. If potential differences between similar systems are the main interest (as is likely the case for most of the studies in the future), these second-order corrections, which are computationally costly to obtain, can be omitted for all practical purposes. The use of the high-quality basis set is crucial to obtain accurate electron attachment energies, which in turn affords quantitative agreement with experimental redox potentials. We presented evidence that the differential solvation energies computed using the continuum solvation model and four different solvents common in electrochemical experiments (H_2O, acetonitrile, DMF, and dichloromethane) is not likely the source of a serious error.

As was briefly discussed above, it is likely that our results could be improved with regard to absolute redox potential via reoptimization of the some of the parameters in the dielectric continuum model. This requires a careful, systematic study of a wide variety of compounds to avoid overfitting, as well as obtaining insight into the physical basis of the deviations that have been observed. Progress along these lines is certainly possible and efforts directed in this fashion are ongoing in our laboratory.

Acknowledgment. This work was supported by grants from the DOE to R.A.F. (Grant DE-FG02-90ER-14162).

Supporting Information Available: Coordinates and energies of all calculations reported herein, calculated vibrational frequencies, energy components (PDF). This material is available free of charge via the Internet at http://pubs.acs.org.

References and Notes

(1) Milazzo, G.; Caroli, S. *Tables of Standard Electrode Potentials*; Wiley: New York, 1977.

(2) Bard, A. J.; Parsons, R.; Jordan, J. *Standard Potentials in Aqueous Solution*; M. Dekker: New York, 1985.

(3) Antelman, M. S. *The Encyclopedia of Chemical Electrode Potentials*; Plenum Press: New York, 1982.

(4) Bard, A. J.; Faulkner, L. R. *Electrochemical Methods*; John Wiley & Sons: New York, 1980.

(5) Balzani, V.; Juris, A.; Venturi, M.; Campagna, S.; Serroni, S. *Chem. Rev.* **1996**, *96*, 759.

(6) Astruc, D. *Electron Transfer and Radical Processes in Transition-Metal Complexes*; VCH: New York, 1995.

(7) Messerschmidt, A.; Huber, R.; Poulos, T.; Wieghardt, K. *Handbook of Metalloproteins*; John Wiley & Sons, Ltd: Chichester, U.K., 2001.

(8) Feig, A. L.; Lippard, S. J. *Chem. Rev.* **1994**, *94*, 759.

(9) Baik, M.-H.; Silverman, J. S.; Yang, I. V.; Ropp, P. A.; Szalai, V. A.; Yang, W. T.; Thorp, H. H. *J. Phys. Chem. B* **2001**, *105*, 6437.

(10) Gill, P. M. W.; Johnson, B. G.; Pople, J. A.; Frisch, M. J. *Int. J. Quantum Chem.: Quantum Chem. Symp.* **1992**, *26*, 319.

(11) Parr, R. G.; Yang, W. *Density Functional Theory of Atoms and Molecules*; Oxford University Press: New York, 1989.

(12) Ziegler, T. *Chem. Rev.* **1991**, *91*, 651.

(13) Slater, J. C. *Quantum Theory of Molecules and Solids, Vol. 4: The Self-Consistent Field for Molecules and Solids*; McGraw-Hill: New York, 1974.

(14) Becke, A. D. *J. Chem. Phys.* **1993**, *98*, 5648.

(15) Becke, A. D. *Phys. Rev. A* **1988**, *38*, 3098.

(16) Lee, C. T.; Yang, W. T.; Parr, R. G. *Phys. Rev. B* **1988**, *37*, 785.

(17) Vosko, S. H.; Wilk, L.; Nusair, M. *Can. J. Phys.* **1980**, *58*, 1200.

(18) Friedrichs, M.; Zhou, R. H.; Edinger, S. R.; Friesner, R. A. *J. Phys. Chem. B* **1999**, *103*, 3057.

(19) Edinger, S. R.; Cortis, C.; Shenkin, P. S.; Friesner, R. A. *J. Phys. Chem. B* **1997**, *101*, 1190.

(20) Marten, B.; Kim, K.; Cortis, C.; Friesner, R. A.; Murphy, R. B.; Ringnalda, M. N.; Sitkoff, D.; Honig, B. *J. Phys. Chem.* **1996**, *100*, 11775.

(21) Cramer, C. J., Truhlar, D. G., Eds. *Structure and Reactivity in Aqueous Solution*; ACS Symposium Series 568; American Chemical Society: Washington, DC, 1994.

(22) Tomasi, J.; Persico, M. *Chem. Rev.* **1994**, *94*, 2027.

(23) Cramer, C. J.; Truhlar, D. G. *Chem. Rev.* **1999**, *99*, 2161.

(24) Patterson, E. V.; Cramer, C. J.; Truhlar, D. G. *J. Am. Chem. Soc.* **2001**, *123*, 2025.

(25) Winget, P.; Weber, E. J.; Cramer, C. J.; Truhlar, D. G. *Phys. Chem. Chem. Phys.* **2000**, *2*, 1231.

(26) Stevens, N. P. C.; Gooch, K. A.; Fisher, A. C. *J. Phys. Chem. B* **2000**, *104*, 1241.

(27) Qiu, F. L.; Williams, N. A.; Fisher, A. C. *Electrochem. Commun.* **1999**, *1*, 124.

(28) Fulian, Q.; Fisher, A. C. *J. Phys. Chem. B* **1998**, *102*, 9647.

(29) Baik, M.-H.; Ziegler, T.; Schauer, C. K. *J. Am. Chem. Soc.* **2000**, *122*, 9143.

(30) Ni, Y. Z.; Rulkens, R.; Manners, I. *J. Am. Chem. Soc.* **1996**, *118*, 4102.

(31) Foucher, D. A.; Ziembinski, R.; Tang, B. Z.; Macdonald, P. M.; Massey, J.; Jaeger, C. R.; Vancso, G. J.; Manners, I. *Macromolecules* **1993**, *26*, 2878.

(32) Schoonover, J. R.; Ni, J. F.; Roecker, L.; Whiter, P. S.; Meyer, T. J. *Inorg. Chem.* **1996**, *35*, 5885.

(33) Hurst, J. K.; Zhou, J. Z.; Lei, Y. B. *Inorg. Chem.* **1992**, *31*, 1010.

(34) Geselowitz, D.; Meyer, T. J. *Inorg. Chem.* **1990**, *29*, 3894.

(35) Ruttinger, W.; Dismukes, G. C. *Chem. Rev.* **1997**, *97*, 1.

(36) ΔG^{EA}(GP) = free energy of electron attachment in gas phase; ΔG^{solv} = difference of solvation free energy; ΔH^{EA}(GP) = gas-phase electron attachment enthalpy; $T\Delta S$(GP) = thermal entropy correction in gas phase; ΔH^{EA}(SCF) = electronic enthalpy computed in the self-consistent-field calculation; ZPE = zero-point-energy correction; $H^T = \int C_p \, dT$ = thermal enthalpy correction; C_p = heat capacity.

(37) Rashin, A. A.; Honig, B. *J. Phys. Chem.* **1985**, *89*, 5588.

(38) *Jaguar 4.1*; Schrödinger, Inc.: Portland, OR, 2000.

(39) Hay, P. J.; Wadt, W. R. *J. Chem. Phys.* **1985**, *82*, 270.

(40) Wadt, W. R.; Hay, P. J. *J. Chem. Phys.* **1985**, *82*, 284.

(41) Hay, P. J.; Wadt, W. R. *J. Chem. Phys.* **1985**, *82*, 299.

(42) Dunning, T. H. *J. Chem. Phys.* **1989**, *90*, 1007.

(43) Computing the vibrational frequencies of all five species of Ru(bpy)$_3^x$—a 63-atom molecule—was technically demanding. Each calculation required ~40 days of CPU time on a Pentium-III/1.2 GHz workstation (Solaris 8).

(44) Lide, D. R. *Handbook of Chemistry and Physics*, 74th ed.; CRC Press: Boca Raton, FL, 1994.

(45) Reiss, H.; Heller, A. *J. Phys. Chem.* **1985**, *89*, 4207.

(46) Alternatively, one could envision partitioning the free energy of solvation into its enthalpic and entropic part and adding only the solvation enthalpy, which would give a physically meaningful term. However, such a partitioning is highly nontrivial and not possible in the continuum solvation model framework.